ROMANIAN JOURNAL OF INFORMATION SCIENCE AND TECHNOLOGY
Volume **14**, Number 3, 2011, 232–241

A Continuous Chaos Generator Using Harmonic Oscillator Circuit

Cristian NEACŞU[1], Valentin CHESARU[1],
Claudius DAN[2], Mircea BODEA[2]

[1]O2 Micro, Romania, Blvd. Vasile Milea nr. 2F, 061344 Bucharest, Romania
E-mail: cr_neacsu@yahoo.com, vali_chesaru@yahoo.com

[2]"POLITEHNICA" University of Bucharest, Romania
E-mail: claudius_dan@yahoo.co, mirceabodea@yahoo.com

Abstract. This paper presents a continuous time chaos generator based on a simple oscillator structure. The developed mathematical model (based on dedicated software), Spice simulation and hardware implementation of the circuit demonstrate the strange attractor and chaotic behavior.

1. Introduction

From the first realizations of electrical circuits that generates chaotic signals, the number and diversity of such circuits grow as much as the interest of scientist on studying this relative new field.

The circuits' inventors generally focused on the most "simple" structure that is able to generate chaos; simple from the perspective (i) of hardware (number of components), (ii) of modeling (nonlinearities characteristics) or (iii) of mathematical analysis. Others just looked for chaotic responses in unexpected situations.

The paper is focused on determining if and when chaos occurs in a harmonic oscillator due to a simple amplitude control circuit of the output periodic signal.

This circuit is not necessarily the most "simple" (it contains an analog multiplexer and has two nonlinearities) but it can present some practical situations involving harmonic oscillators.

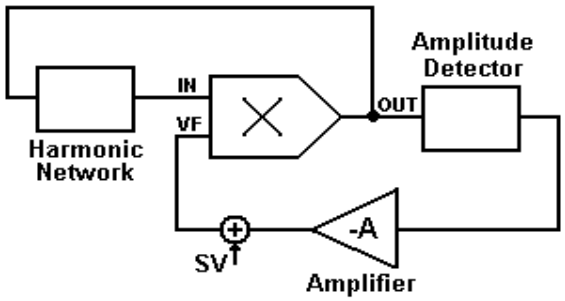

Fig. 1. Harmonic oscillator with amplitude controller.

The oscillator block diagram is presented in Fig. 1. There are two feedback loops: the positive one, which includes the harmonic network, and creates the oscillation signal and the negative one which stabilizes the amplitude of the sinusoidal output.

2. Circuit description

The detailed schematic of the Fig. 1 oscillator is presented in Fig. 2. For simplicity the circuit's operation is examined by sweeping only one parameter, namely the SV feedback offset.

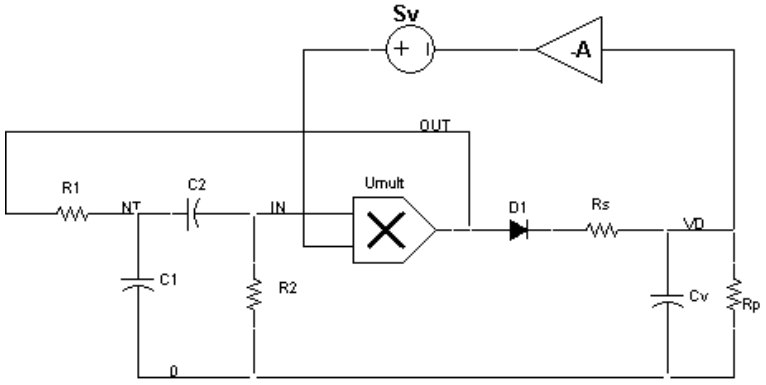

Fig. 2. The chaotic oscillator circuit.

The circuit's component and parameters values are:

$$R_1 = R_2 = 1\ \text{k}\Omega,\quad C_1 = C_2 = 10\ \text{nF},$$
$$R_S = 1\ \text{k}\Omega,\quad R_P = 7\ \text{k}\Omega,\quad C_V = 30\ \text{nF},$$
$$A_V = 3,\quad S_V = 4 \ldots 8\text{V},$$
$$I_S = 2.5\ \text{nA},\quad V_{th} = 25\ \text{mV},\quad \sigma_V = 1\ \text{V}$$

The circuit behavior is described by three differential equations; two introduced by the harmonic network, equations (1) and (2), and one by the amplitude detector, equation (3):

$$\frac{OUT - V_{C1}}{R_1} = C_1 \dot{V}_{C1} + \frac{IN}{R_2}, \tag{1}$$

$$\frac{IN}{R_2} = C_2 \dot{V}_{C2}, \tag{2}$$

$$I_D = C_V \cdot \dot{V}_D + \frac{V_D}{R_P}, \tag{3}$$

and by

$$V_{C1} = V_{C2} + IN, \tag{4}$$

$$OUT = IN \cdot (S_V - A_V V_D)/\sigma_V, \tag{5}$$

$$I_D = I_S \left[\exp \frac{OUT - V_D - I_D R_S}{V_{th}} - 1 \right], \tag{6}$$

where the nodes name corresponds to Fig. 2 schematic. In order to make the circuit's analysis simpler the capacitors' voltages are taken as variables, [2].

3. The circuit analysis

The circuit has three capacitors and no loop with multiple initial states, so one can say that the physical phase space has three dimensions (initial condition is completely determined by three numbers).

The canonical form of the circuit equations results from (1)–(6):

$$\dot{V}_{C1} = f_1 (V_{C1}, V_{C2}, V_D) = \frac{1}{R_1 C_1} \left[(V_{C1} - V_{C2}) \left(\frac{S_V - A_V V_D}{\sigma_V} - \frac{R_1}{R_2} \right) - V_{C1} \right]$$

$$\dot{V}_{C2} = f_2 (V_{C1}, V_{C2}, V_D) = \frac{1}{R_2 C_2} (V_{C1} - V_{C2}) \tag{7}$$

$$\dot{V}_D = f_3 (V_{C1}, V_{C2}, V_D) = \frac{1}{R_P C_V} \left[R_P \left(\frac{V_{th}}{R_S} W(\xi) - I_S \right) - V_D \right]$$

where $W(x)$ is the Lambert function defined by:

$$x = W(x) \cdot e^{W(x)}, \tag{8}$$

and

$$\xi = \frac{I_S R_S}{V_{th}} \exp \left[\frac{1}{V_{th}} \left(\frac{(V_{C1} - V_{C2})(S_V - A_V \cdot V_D)}{\sigma_V} + I_S R_S - V_D \right) \right]. \tag{9}$$

The fixed point can be found by solving the system of equations:

$$\begin{aligned} f_1(V_{C1}, V_{C2}, V_D) &= 0; \\ f_2(V_{C1}, V_{C2}, V_D) &= 0; \\ f_3(V_{C1}, V_{C2}, V_D) &= 0. \end{aligned} \tag{10}$$

It can be easily calculated that the circuit has only one fixed point, the origin:

$$V_{C1} = 0, \;\; V_{C2} = 0, \;\; V_D = 0. \tag{11}$$

In order to evaluate the nature of this fixed point and to determine the dissipation value of the circuit, the Jacobian matrix and its eigenvalues are calculated:

$$\begin{aligned} \frac{\partial f_1}{\partial V_{C1}} &= \frac{1}{R_1 C_1}\left(\frac{V_F}{\sigma_V} - \frac{R_1}{R_2} - 1\right) \frac{\partial f_2}{\partial V_{C1}} = \frac{1}{R_2 C_2} \frac{\partial f_3}{\partial V_{C1}} = \frac{1}{R_P C_V} \frac{V_F}{\sigma_V} D_W(\xi) \\ \frac{\partial f_1}{\partial V_{C2}} &= \frac{-1}{R_1 C_1}\left(\frac{V_F}{\sigma_V} - \frac{R_1}{R_2}\right) \frac{\partial f_2}{\partial V_{C2}} = \frac{-1}{R_2 C_2} \frac{\partial f_3}{\partial V_{C2}} = \frac{-1}{R_P C_V} \frac{V_F}{\sigma_V} D_W(\xi) \end{aligned} \tag{12}$$

$$\frac{\partial f_1}{\partial V_D} = \frac{-A_V}{R_1 C_1} \frac{V_{C1} - V_{C2}}{\sigma_V} \frac{\partial f_2}{\partial V_D} = 0 \frac{\partial f_3}{\partial V_D} = \frac{-1}{R_P C_V} \left[\left(1 + A_V \frac{V_{C1} - V_{C2}}{\sigma_V}\right) D_W(\xi) + 1 \right]$$

where

$$D_W(\xi) = \frac{R_P}{R_S} \frac{W(\xi)}{1 + W(\xi)}. \tag{13}$$

In the calculation of those formulas, it was used the known result that can be easily derived from equation (5):

$$W'(x) = \frac{W(x)}{1 + W(x)} \frac{1}{x}. \tag{14}$$

The eigenvalues corresponding to the fixed point are:

$$\begin{aligned} \lambda_1 &= \frac{1}{R_1 C_1} \left[\chi + \sqrt{\chi^2 - \frac{R_1 C_1}{R_2 C_2}} \right], \\ \lambda_2 &= \frac{1}{R_1 C_1} \left[\chi - \sqrt{\chi^2 - \frac{R_1 C_1}{R_2 C_2}} \right], \\ \lambda_3 &= \frac{-1}{R_P C_V} \left[\frac{I_S (R_S + R_P) + V_{th}}{I_S R_S + V_{th}} \right], \end{aligned} \tag{15}$$

where

$$\chi = \frac{1}{2} \left(\frac{S_V}{\sigma_V} - \frac{R_1 C_1}{R_2 C_2} - \frac{R_1}{R_2} - 1 \right). \tag{16}$$

We remind that divergence defined by:

$$div(f) = \frac{\partial f_1}{\partial V_{C1}} + \frac{\partial f_2}{\partial V_{C2}} + \frac{\partial f_3}{\partial V_D} \tag{17}$$

measures how fast the trajectory approaches the attractor (in the case of dissipative systems when *div* is negative).

To proper characterize the system dynamics, the divergence should be calculated as a mean over a large number of point distributed uniformly along the attractor. Using previous results, it was calculated the mean divergence value (from a large data set) and the eigenvalues of the fixed point for some S_V parameter values:

S_V [V]	λ_1 [1/µs]	λ_2 [1/µs]	λ_3 [1/µs]	*div* [V/ms]
2.8	$-0.1 + 0.099$i	$-0.1 - 0.099$i	-0.0047	-24.76
3	$0 + 0.1$i	$0 - 0.1$ i	-0.0047	-4.76
4.8	$0.09 + 0.043$i	$0.09 - 0.043$i	-0.0047	-21.65
5	0.1000	0.1000	-0.0047	-22.44
6.2	0.2849	0.0351	-0.0047	-17.56
6.5	0.3186	0.0313	-0.0047	-20.68
7	0.3732	0.0267	-0.0047	-22.50
7.5	0.4265	0.0234	-0.0047	-22.14

The nature of the fixed point, [1], can be summarized as follows:

$S_V < 3$	Attracting point
$3 < S_V < 5$	Spiral saddle point index-2
$S_V > 5$	Saddle point index-2

Index-2 means that the trajectories:

- approach the saddle point on a curve and diverge on a surface – for all real eigenvalues (two positive, one negative) or
- are spiral around the saddle point on a surface as they diverge – for two complex eigenvalues with positive real part and one negative real.

4. Results

To check that the system shows bifurcation phenomena and chaotic behavior its operation was simulated for S_V values ranging from 5 to 7.5.

The time and phase space diagram for few S_V values are presented below. Figure 3 corresponds to a near harmonic oscillation (only one dominant frequency). Signals in time are near sinusoids and the trajectory in phase space is a closed curve with one turn: this is the case for low S_V values.

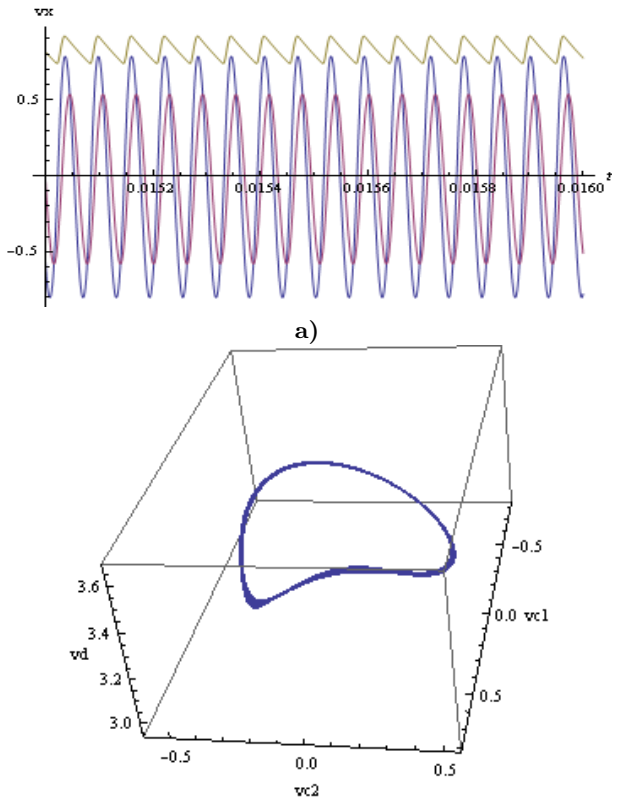

Fig. 3. V_{C1} (blue), V_{C2} (violet) and V_D (green) signals vs. time, (a), and phase space, (b), diagram for $S_V = 5.5$ V.

Figure 4 presents a double frequency oscillation – the local amplitude signal changes consecutively between two values and the trajectory in phase space is a closed curve with two turns: this case correspond of a medium value of S_V (after a first bifurcation event occurred).

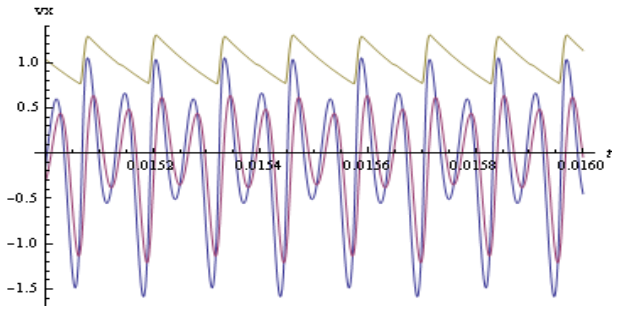

Fig. 4a. V_{C1} (blue), V_{C2} (violet) and V_D (green) signals vs. time diagram for $S_V = 6.1$ V.

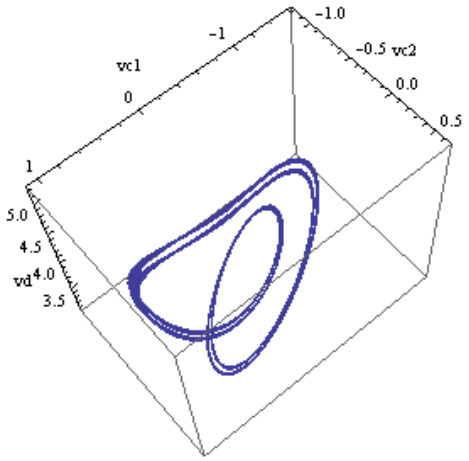

Fig. 4b. V_{C1}, V_{C2} and V_D phase space diagram for $S_V = 6.1$ V.

Figure 5 describes a chaotic oscillation (with a broadband spectrum) – the signal has a random like aspect (in the long term the signal evolution cannot be predicted); the trajectory in phase space does not close itself and it is distributed in a large volume.

Further information about chaotic dynamics can be obtained from Poincaré sections. A periodic signal will be characterized by a Poincaré section formed only by points. A trajectory that attracts toward a torus (this kind of signal is not periodic but not chaotic) is characterized by a closed curve in the Poincaré diagram. A chaotic signal generates a fractal in the Poincaré diagram.

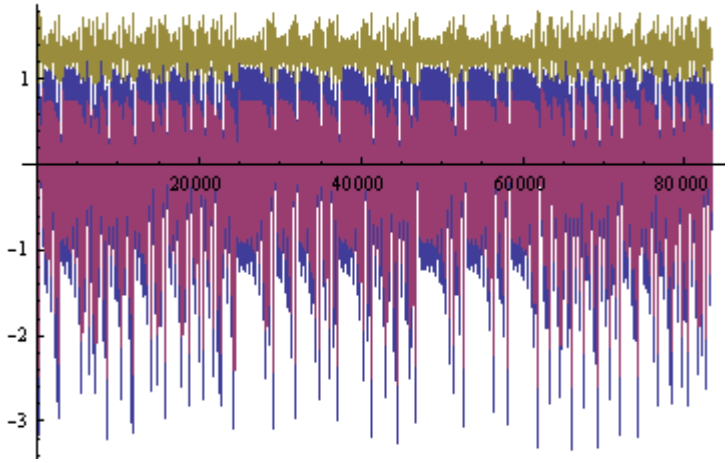

Fig. 5a. V_{C1} (blue), V_{C2} (violet) and V_D (green) signals vs. time for $S_V = 7$ V.

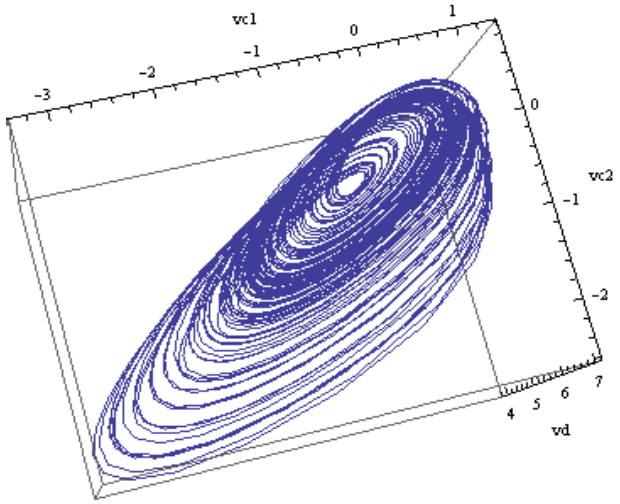

Fig. 5b. V_{C1}, V_{C2} and V_D phase space diagram for $S_V = 7$ V.

The Poincaré diagrams of the generated signals (see Fig. 6) presents multiple sections for various S_V. It can be noted that for small S_V the section contains only 2 points (corresponding to a closed trajectory after a first bifurcation). Finally, for large S_V the circuit operates in chaotic domain as results from the two crossing zones zoom; it can be seen the substructure formed – sign of a fractal geometry.

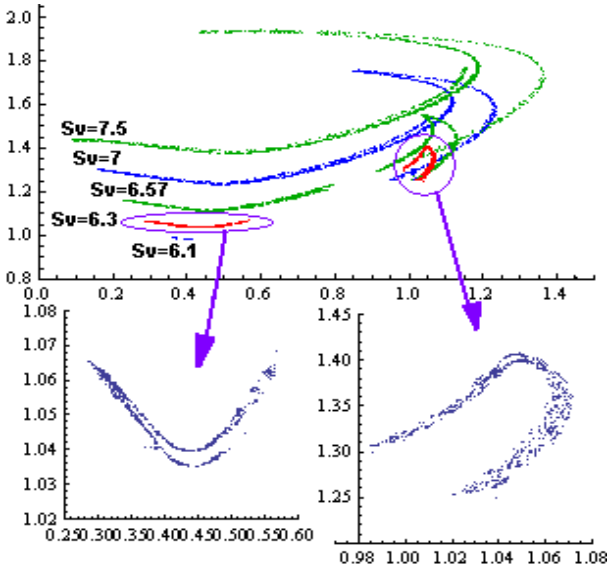

Fig. 6. Poincaré sections for various S_V values and zoom of the significant details for $S_V = 6.3$ V.

The previous results were verified by Spice simulation. Figure 7 presents the time diagram and a FFT spectrum for the chaotic domain ($S_V = 7$ V) operation.

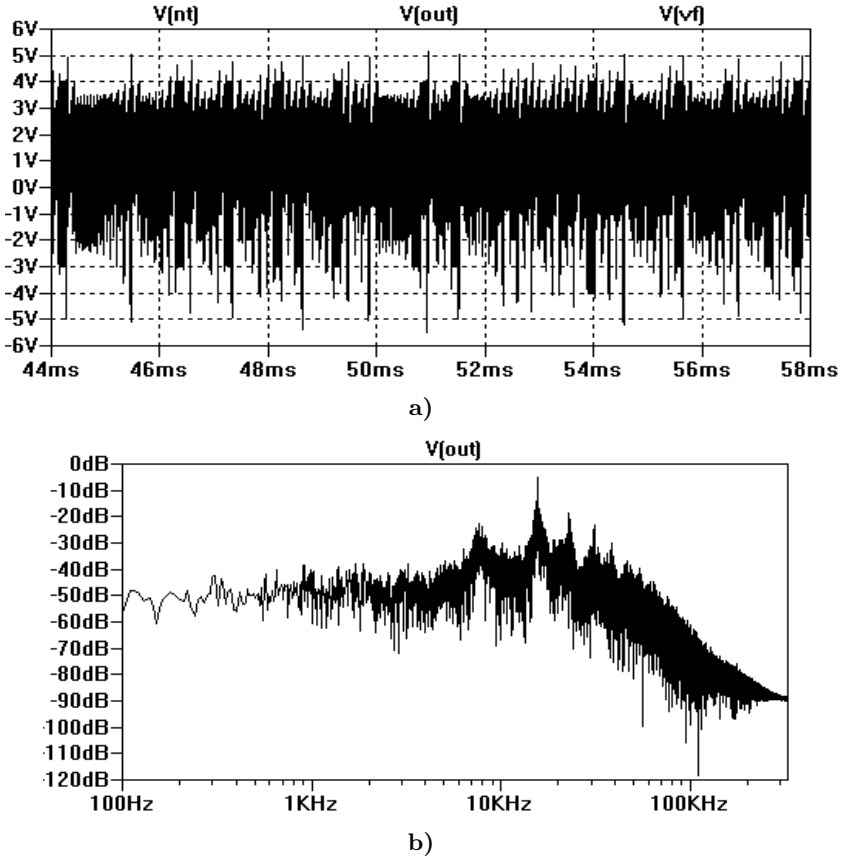

Fig. 7. NT, OUT and VF nodes voltages versus time, (a), and FFT of the OUT node voltage, (b), obtained with LTSpice.

The chaotic nature of this circuit was further studied by measuring the largest Lyapunov exponent. The method used to estimate this parameter was the one described in [3] in which it is used the synchronization of two identical systems (with different initial conditions); the largest Lyapunov exponent measured for different S_V parameter are presented in Fig. 8.

The scope view of the chaotic operation of the Fig. 2 circuit is presented in Fig. 9, which display NT vs. OUT signals.

5. Conclusion

This paper presented a detailed study of an autonomous chaos generator made by a simple oscillator configuration with a strong negative feedback on the amplitude stabilization circuitry.

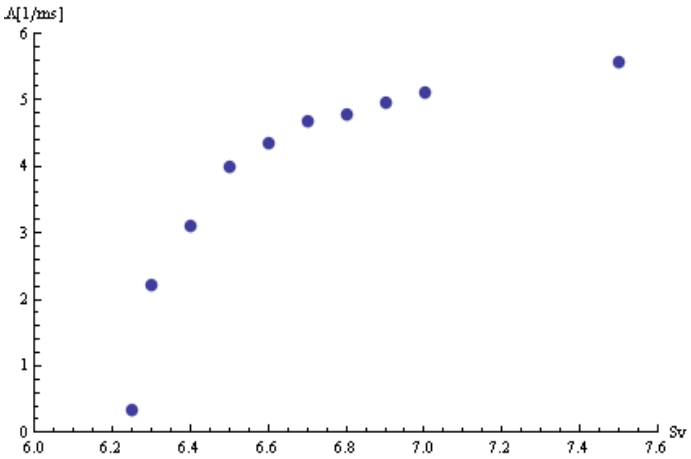

Fig. 8. Largest Lyapunov exponent versus S_V parameter.

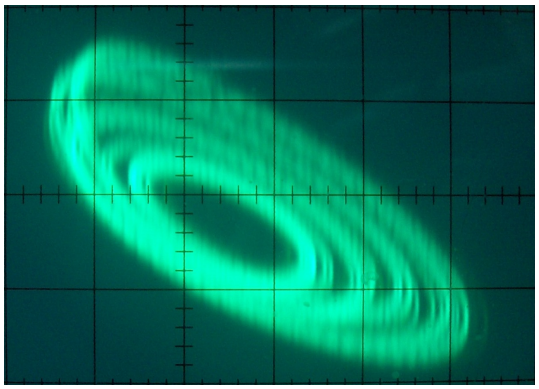

Fig. 9. NT (vertical, 500 mV/div) versus OUT (horizontal, 1 V/div) of Fig. 2 circuit.

References

[1] Hilborn R.C., *Chaos and Nonlinear Dynamics – An Introduction for Scientists and Engineers*, Oxford University Press, 2000.

[2] De Feo O., Maggio G.M., *Bifurcations in the Colpitts Oscillator: From Theory to Practice*, International Journal of Bifurcation and Chaos, Vol. **13**, No. 10, 2003.

[3] Stefanski A., Kapitaniak T., *Using Chaos Synchronization to Estimate the Largest Lyapunov Exponent of Nonsmooth Systems*, Discrete Dynamics in Nature and Society, Vol. **4**, pp. 207–215, 1999.